ARTICLE NO. 79-4093

Finite-Element Approach to Compressor Blade-to-Blade Cascade Analysis

Wagdi G. Habashi*
Concordia University, Montreal, Quebec, Canada
and
Ernest G. Dueck† and David P. Kenny‡
Pratt and Whitney Aircraft of Canada Ltd., Longueuil, Quebec, Canada

A study of the application of the finite-element method to compressible potential flows in the context of axial turbomachinery is undertaken. Some novel finite-element approaches relating to the analysis as well as to the mesh generation are presented. The solutions use a pseudovariational integral, applicable to shockless transonic flows and possessing a physical basis for the iteration. Appropriate grids are generated automatically for all cascades at any solidity. The scheme is based upon an approximate mapping of a blade into a near circle around which a suitable grid, with layers reproducing the airfoil shape, is constructed. Such mapping homogenizes the gradients by geometrically condensing regions of low gradients on the main part of the blade while magnifying regions of steep gradients near the leading and trailing edges. The analysis, however, is carried out in the original physical plane. Successful comparisons are made with other results for incompressible and compressible flows.

Nomenclature

a = speed of sound
F = right-hand side of finite element matrix equation
I = variational integral
k = influence matrix, on an element basis
K = influence matrix on a global assembly basis
m = meridional distance
M = Mach number with respect to stagnation speed of sound
n = outward normal direction to a boundary
p = pressure
r,t = local normalized coordinates within elements
R = radius of streamtube
s = pitch in radians, $2\pi/$(number of blades)
u,v = velocity components in m and θ directions, respectively
β = flow angle
γ = isentropic exponent
δ = a variation
θ = circumferential distance measured from bottom left of selected solution domain (Fig. 1)
ξ_e,η_e = local velocity direction in element e and its normal, respectively
ρ = density
σ = velocity direction in an element with respect to m axis
ϕ,Φ = velocity potential
[ ] = matrix
{ } = vector
⌊ ⌋ = transpose of a vector

Subscripts

i = property at nodal point i
0 = stagnation property
(in) = property at channel inlet
(ex) = property at channel exit
(e) = property of element e

Received June 30, 1978; revision received Jan. 8, 1979.

Index categories: Computational Methods; Transonic Flow; Aerodynamics.

*Associate Professor, Mechanical Engineering Dept. Member AIAA.
†Staff Aerodynamics Engineer.
‡Manager, Rotating Components, Aerodynamics.

Introduction

THE problem of developing calculation procedures for subsonic or transonic inviscid flows in the context of turbomachinery has received considerable attention in the past.[1-6] Finite-difference (FD or FDM) approaches have been considered to be the most reliable and economical.

Katsanis[1,2] has obtained solutions to high subsonic cascades using the stream function approach. McDonald[3] and Denton[4] use a time marching approach for which a finite area method is utilized to obtain the nodal equations. While the method handles all three flow regimes with ease, its convergence speeds are rather slow if only transonic flows are of interest.

Another alternative has been proposed by Ives and Liutermoza[5,6] who formulate a second-order finite-difference approach to supercritical flows after mapping the cascade onto the inside of a bounded rectangular region. The required mappings are strongly a function of the problem at hand and do not seem to provide accurate solutions for blades with rounded trailing edges. Results have been presented only for low solidity (chord/pitch <1) cascades, since such mappings are usually a strong function of cascade solidity.

Recently, the finite-element method (FE or FEM) has received attention as a potential candidate for such problems. Model finite-element problems of incompressible inviscid flows around bodies have been presented by Martin,[7] Chan and Larock,[8] and Argyris,[9] among others. The extension of these approaches to the nonlinear compressible flows over isolated airfoils or cascades has in many cases been facilitated by developments that utilize linearization processes.[9-14] In the present paper, a pseudovariational principle is applied to the blade-to-blade flow equation for cascade channels.

Governing Equations

For the blade-to-blade channel of a compressor cascade, defining m as the meridional flow direction and θ as the circumferential direction, the steady-state Navier Stokes inviscid, compressible flow governing equations can be written as:

Continuity

$$\frac{\partial}{\partial m}[\rho u]+\frac{1}{r}\frac{\partial}{\partial \theta}[\rho v]=0 \tag{1}$$

m momentum

$$\frac{\partial}{\partial m}[p+\rho v^2]+\frac{1}{r}\frac{\partial}{\partial \theta}[\rho uv]=0 \tag{2a}$$

θ momentum

$$\frac{\partial}{\partial m}[\rho uv]+\frac{1}{r}\frac{\partial}{\partial \theta}[p+\rho v^2]=0 \tag{2b}$$

Energy or isentropic relation

$$p/\rho^{\gamma}=\text{constant} \tag{3}$$

With the weak shock assumption, and hence in the absence of any vorticity generation, the potential ϕ is introduced in the usual way and one obtains

$$(a^2-v^2)\Phi_{mm}-2\frac{uv}{r}\Phi_{m\theta}+\frac{1}{r^2}(a^2-v^2)\Phi_{\theta\theta}=0 \tag{4a}$$

with

$$a^2=a_0^2-\left(\frac{\gamma-1}{2}\right)(\nabla\Phi)^2 \tag{4b}$$

or alternatively,

$$\frac{\partial}{\partial m}\left[\rho\frac{\partial\Phi}{\partial m}\right]+\frac{1}{r}\frac{\partial}{\partial\theta}\left[\frac{\rho}{r}\frac{\partial\Phi}{\partial\theta}\right]=0 \tag{5a}$$

$$\frac{\rho}{\rho_0}=\left[1-\frac{\gamma-1}{2a_0^2}(\nabla\Phi)^2\right]^{\frac{1}{\gamma-1}} \tag{5b}$$

a_0, ρ_0 being the stagnation speed of sound and the stagnation density, respectively, and γ the ratio of the specific heats. Equations (5a) and (5b) are adopted in this work because of their simpler form and their special adaptability to a FE variational formulation.[11-14]

Local Linearization Analysis

The local linearization approach in finite elements[12,13] recognizes the localized capabilities inherent in the method. In case of nonlinear equations, it is possible to linearize the equations with respect to a mean flow parameter such as the freestream Mach number for example. Since the finite-element discretization only requires a locally valid equation, it is hence permissible to perform a different linearization in each element, with regard to the local Mach number in the element.

Assuming an initial potential distribution for the entire flowfield provides within each element a flow of velocity V_e, Mach number M_e, and density ρ_e. Let local Cartesian coordinates (ξ_e, η_e) (Fig. 2) be defined along V_e and its normal, respectively, within each element. The variational equivalent $I(\phi)$ of Eq. (5a) can be evaluated over the elements as

$$I(\Phi)=\sum_{e=1}^{N} I^{(e)}(\Phi) \tag{6}$$

Assuming the next iterative step to consist of a perturbation flow within each element around V_e gives

$$v_e^{(n+1)}=[V_e^{(n)}+u';v'] \tag{7}$$

where u'/V_e, $v'/V_e \ll 1$ and $\Phi=V_e\xi_e+\phi'(\xi_e,\eta_e)$.

The perturbation potential is governed by the Prandtl-Glauert equation

$$\rho_e\left[(1-M_e^2)\frac{\partial^2\phi'}{\partial\xi_e^2}+\frac{\partial^2\phi'}{\partial\eta_e^2}\right]=0 \tag{8}$$

for which the stretching $\xi_e'=\xi_e/\sqrt{1-M_e^2}$, $\eta_e'=\eta_e$, gives the Laplace equation with regard to ξ_e', η_e'. The applicable variational principle can be written immediately as

$$\delta I^{(e)}(\phi')=\frac{1}{2}\delta\int_{A_e'}\int\rho_e[\nabla'\phi']^2 d\xi_e' d\eta_e'$$

$$-\oint_{C_e'}\rho\delta\phi'\left(\frac{\partial\phi'}{\partial n_e'}\right)ds_e' \tag{9}$$

Reconverting into global variables and insuring the cancellation of the contour integral over the edges of adjacent elements, the derived variational integral then becomes

$$\delta I(\Phi)=\frac{1}{2}\delta\sum_{e=1}^{N}\rho_e\int_{A_e}\int[(1-M_e^2)\Phi_{\xi_e}^2+\Phi_{\eta_e}^2$$

$$+2V_eM_e^2\Phi_{\xi_e}]d\xi_e d\eta_e-\oint_C\rho\delta\left(\frac{\partial\Phi}{\partial n}\right)ds \tag{10}$$

This variational integral provides the basis for an iterative procedure where at each step new values of V_e, M_e, ρ_e as well as a new ξ_e direction are obtained.

The preceding equation may be rewritten as

$$\delta I(\Phi)=\left[\frac{\delta}{2}\sum_{e=1}^{N}I_1(\Phi)\right]+\delta I_2(\Phi) \tag{11}$$

where $I_2(\Phi)$ applies only to elements on the outer contour of the domain analyzed, (C).

The physical iterative basis inherent in the formulation of this variational principle speeds up, as well as guarantees, convergence for all subsonic Mach numbers. The $(1-M_e^2)$ coefficient which appears naturally in the formulation helps smooth the solution in the sensitive transitional transonic pockets present in these flows.

Boundary Conditions for Cascade Flows

Assume that the inlet and exit angles β_{in}, β_{ex} are given and defined as shown in Fig. 1. Also given are M_{in}, P_0, T_0, γ, and, hence, a_0 and ρ_0, the stagnation properties of the flow. If we define the pitch as s and the radius of the blade-to-blade section as R, we have on

$$A-B:\quad \Phi(\theta)=[Ra_0(M_{in})\sin(\beta_{in})]\theta+\text{const} \tag{12a}$$

where θ is measured from B. The constant is selected as 0 at point B. Although the specification of R is superfluous for a cylindrical stream surface, it is retained in the equations to permit extension to arbitrary stream surfaces.

$$B-C:\quad \Phi=\Phi_1(m);\quad \text{unknown} \tag{12b}$$

$$D-E:\quad \Phi=\Phi_2(m);\quad \text{unknown} \tag{12c}$$

$A-H$ and $G-F$ are periodic boundaries separated from $B-C$ and $D-E$ by one pitch, hence on

$$A-H:\quad \Phi(m)=\Phi_1(m)+a_0Rs(M_{in})\sin\beta_{in} \tag{12d}$$

$$G-F:\quad \Phi(m)=\Phi_2(m)+a_0Rs(M_{ex})\sin\beta_{ex} \tag{12e}$$

where M_{in} and M_{ex} are the inlet and exit Mach numbers, respectively, defined with respect to the stagnation speed of sound.

$$C-D \text{ and } H-G:\quad \partial\Phi/\partial n=0 \tag{12f}$$

where n is the outward normal to the blade surface at each point.

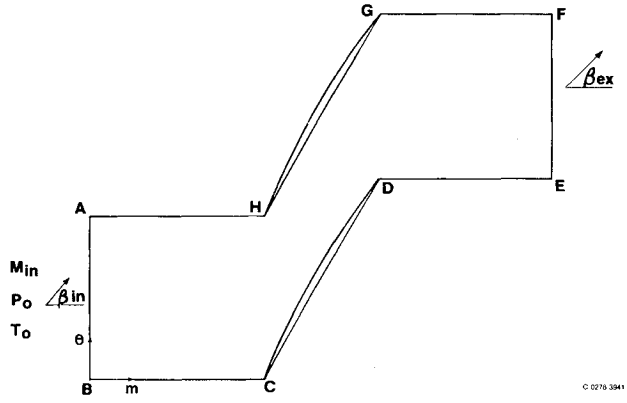

Fig. 1 Solution domain and boundary conditions.

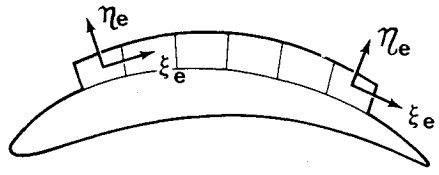

Fig. 2 Eight-node isoparametric element and local elemental coordinates, with test blade, after splining.

$E-F$: only the axial exit speed is defined

$$\partial\Phi/\partial n = (M_{ex}) \cdot a_0 \cos\beta_{ex} \tag{12g}$$

where M_{ex} is obtained by conservation of mass, i.e.,

$$\dot{w} = (M_{ex})\cos\beta_{ex}\rho_{ex} = (M_{in}) \cdot \cos\beta_{in}\rho_{in}$$

giving the mass flow parameter

$$\frac{\rho_{ex}}{\rho_0} M_{ex} = \frac{\rho_{in}}{\rho_0} M_{in} \frac{\cos\beta_{in}}{\cos\beta_{ex}} \tag{12h}$$

To obtain ρ_{ex}/ρ_0 and M_{ex} separately, a Newton-Raphson technique is applied to

$$\frac{\rho_{ex}}{\rho_0} M_{ex} = \left[1 - \frac{\gamma-1}{2}(M_{ex})^2\right]^{\frac{1}{\gamma-1}} M_{ex} = \frac{\rho_{in}}{\rho_0} M_{in} \frac{\cos\beta_{in}}{\cos\beta_{ex}} \tag{13}$$

as in Refs. 1 and 2.

Finite-Element Discretization

The domain in question is subdivided into isoparametric eight-node quadrilateral elements as in Fig. 2. One has, within each element

$$\Phi(m,\theta) = \sum_{i=1}^{8} \Phi_i N_i(r,t) \tag{14}$$

where

$$N_i = \tfrac{1}{4}(1+rr_i)(1+tt_i)(rr_i+tt_i-1) \qquad i=1,3,5,7$$

$$N_i = \tfrac{1}{4}(1+rr_i)(1-t^2t_i^2) \qquad i=4,8$$

$$N_i = \tfrac{1}{4}(1-r^2r_i^2)(1+tt_i) \qquad i=2,6$$

where N_i are the shape functions in the local coordinate system (r,t).[15]

The isoparametric concept also describes the geometry of the element to the same order as the approximating function itself, namely

$$m = \sum_{i=1}^{8} m_i N_i(r,t) \tag{15a}$$

$$\theta = \sum_{i=1}^{8} \theta_i N_i(r,t) \tag{15b}$$

In other words, the geometry of each element can be exactly approximated up to a parabolic variation between points, straight lines being special cases of parabolas. Such a description is useful in the representation of highly cambered turbomachinery blades, especially in leading- and trailing-edge regions.

Minimization of I_1

From Eq. (10) and upon minimization with respect to the nodal values Φ_i, $(i=1,8)$ in each element

$$\frac{\partial}{\partial\{\Phi_i\}}\frac{\partial(\Phi^2)}{\partial\xi} = 2\frac{\partial\Phi}{\partial\xi}\frac{\partial\Phi}{\partial\{\Phi_i\}} = 2\frac{\partial N_i}{\partial\xi}\left(\frac{\partial N_j}{\partial\xi}\Phi_j\right) \tag{16}$$

$$\frac{\partial}{\partial\{\Phi_i\}}\frac{\partial(\Phi^2)}{\partial\eta} = 2\frac{\partial N_i}{\partial\eta}\left(\frac{\partial N_j}{\partial\eta}\Phi_j\right) \tag{17}$$

$$\frac{\partial}{\partial\{\Phi_i\}}\frac{\partial\Phi}{\partial\xi} = \frac{\partial N_i}{\partial\xi} \tag{18}$$

where repeated indices indicate summation, one obtains the element influence matrix coefficients

$$k_{ij} = \rho_e\left[\iint_{A_e}(1-M_e^2)\frac{\partial N_i}{\partial\xi_e}\frac{\partial N_j}{\partial\xi_e} + \frac{\partial N_i}{\partial\eta_e}\frac{\partial N_j}{\partial\eta_e}\right]d\xi_e d\eta_e \tag{19a}$$

and the element contribution to the right-hand side

$$f_i = -\rho_e V_e M_e^2 \iint_{A_e}\frac{\partial N_i}{\partial\xi_e}\,d\xi_e d\eta_e \tag{19b}$$

since all shape functions are in terms of the local coordinates (r,t) one proceeds as follows:

$$\begin{Bmatrix}\frac{\partial N_i}{\partial r}\\ \frac{\partial N_i}{\partial t}\end{Bmatrix} = \begin{bmatrix}\frac{\partial m}{\partial r} & \frac{\partial\theta}{\partial r}\\ \frac{\partial m}{\partial t} & \frac{\partial\theta}{\partial t}\end{bmatrix}\begin{Bmatrix}\frac{\partial N_i}{\partial m}\\ \frac{\partial N_i}{\partial\theta}\end{Bmatrix} = [J]\begin{Bmatrix}\frac{\partial N_i}{\partial m}\\ \frac{\partial N_i}{\partial\theta}\end{Bmatrix} \tag{20}$$

or

$$\begin{Bmatrix}\frac{\partial N_i}{\partial m}\\ \frac{\partial N_i}{\partial\theta}\end{Bmatrix} = [J]^{-1}\begin{Bmatrix}\frac{\partial N_i}{\partial r}\\ \frac{\partial N_i}{\partial t}\end{Bmatrix} \tag{21}$$

and, hence,

$$\begin{Bmatrix}\frac{\partial N_i}{\partial\xi_e}\\ \frac{\partial N_i}{\partial\eta_e}\end{Bmatrix} = \begin{bmatrix}\cos\sigma & \frac{\sin\sigma}{R}\\ -\sin\sigma & \frac{\cos\sigma}{R}\end{bmatrix}^{(e)}\begin{Bmatrix}\frac{\partial N_i}{\partial m}\\ \frac{\partial N_i}{R\partial\theta}\end{Bmatrix} \tag{22}$$

where σ is the local velocity direction, in each element, determined from the previous iteration, namely

$$\sigma^{(e)} = \tan^{-1}\left[\frac{\frac{\partial\Phi}{R d\theta}}{\frac{\partial\Phi}{\partial m}}\right]^{(e)} = \tan^{-1}\frac{\frac{1}{R}\left\lfloor\frac{\partial N_i}{\partial\theta}\right\rfloor\{\Phi i\}^{(e)}}{\left\lfloor\frac{\partial N_i}{\partial m}\right\rfloor\{\Phi i\}} \tag{23}$$

at the centroid.

The influence matrix in Eq. (19a) is formed for each element by a 3×3 numerical Gaussian integration and assembled in a global matrix in the usual fashion,[15]

$$[K]\{\Phi\}=\{F\} \tag{24}$$

The system of algebraic equations is solved using a variable bandwidth modified Cholesky decomposition scheme.

Minimization of I_2

The integral I_2 is zero or cancels out on all surfaces except on $E-F$. Thus,

$$I_2=-\int\rho\delta\Phi\left(\frac{\partial\Phi}{\partial n}\right)R\mathrm{d}\theta=+\rho_{ex}R(M_{ex})a_0s\cos\beta_{ex}\int\delta\Phi\mathrm{d}\theta$$

$$=+\rho_{ex}R(M_{ex})a_0s\cos\beta_{ex}\sum_{e=1}^{N_l}\int_{-l}^{l}N_i\mathrm{d}t\frac{L^{(e)}}{2} \tag{25}$$

where $L^{(e)}$ is the length of the boundary of each element on the exit face $E-F$.

Hence for each element on $E-F$, upon minimization with regard to Φ_3,Φ_4,Φ_5 the following additional vector (F_i) results

$$\{F_i\}=\frac{l}{6}\rho_{ex}R(M_{ex})a_0s\cos(\beta_{ex})L^{(e)}\begin{Bmatrix}0\\0\\1\\4\\1\\0\\0\\0\end{Bmatrix} \tag{26}$$

where the element nodes are ordered counterclockwise starting at bottom left, and the global influence matrix can be rewritten as

$$[K]\{\Phi\}=\{F\}^* \tag{27}$$

where $\{F\}^*$ has been modified to contain the contribution of elements on $E-F$.

Mesh Generation Scheme

In developing a mesh generation scheme, it is to be appreciated that in an industrial context, such an analysis is frequently a daily routine. The program should therefore be simple enough and flexible enough to enable the user to obtain accurate answers without the laborious and time consuming efforts normally associated with FEM grid construction.

In the present work any blade profile is first splined and then fitted with appropriate leading- and trailing-edge circles. Several points are chosen on these circles to insure a faithful representation of these crucial zones. The remaining subdivisions are then chosen along the blade chord in an expanding or contracting fashion according to relative curvature of the blade surface or according to requirements defined by the user. The airfoil is then mapped by a one-step explicit conformal transformation into a near circle around which contiguous layers reproducing the airfoil shape can be generated (Fig. 3). The number of layers and their thickness are parameters of the program. The generated mesh is then mapped back to the physical plane (Fig. 4).

To complete the mesh generation a number of subdivisions are chosen across the pitch, outside of the generated layers, where elements are constructed in an isoparametric fashion

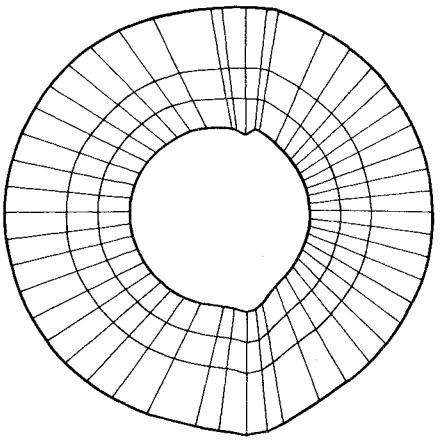

Fig. 3 Blade mapped by conformal transformation into a pseudocircle with generated layers.

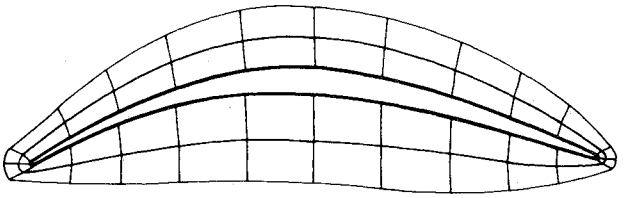

Fig. 4 FE layers around blade, in physical plane.

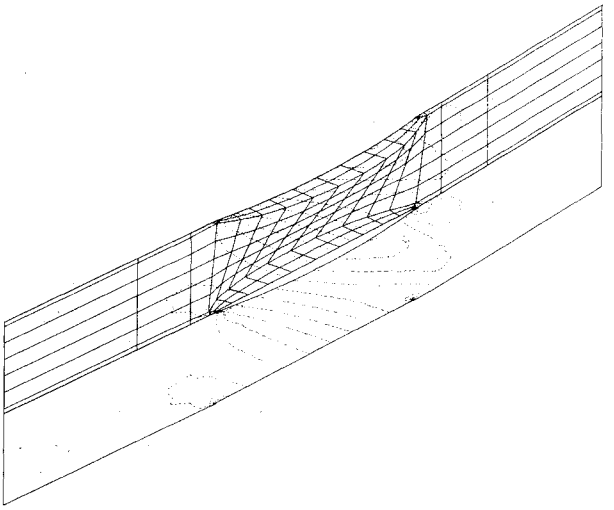

Fig. 5 Overall mesh and Mach number contours of a compressor blade.

(Fig. 5). The density of these elements across the pitch and in the upstream and downstream sections is defined as an input. Furthermore, element sizes in the upstream and downstream regions can be tailored (by contraction or expansion) to accommodate the transition, from uniform flow far upstream or downstream, to the regions of high flow gradients within the cascade. It may also be worthwhile to mention that the blade splining permits the selection of exact midpoints for the isoparametric elements, a fact of considerable importance when such elements are used.

Results and Discussion

Several test cases have been analyzed to verify the application of this method to a spectrum of test cases from incompressible to transonic. Comparisons are made with both exact and analytical results. Figure 6 shows the comparison to an exact solution by Gostelow[16] for the incompressible flow over a compressor blade at a very severe negative incidence of

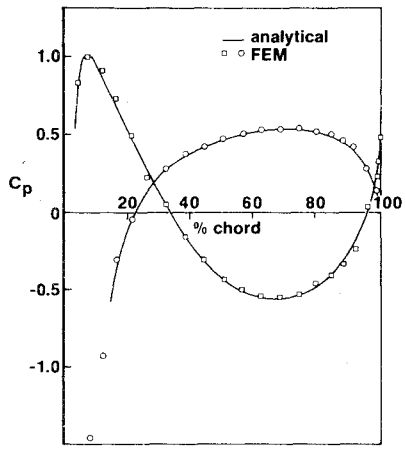

Fig. 6 FEM results and comparison to Gostelow's analytical incompressible solution.

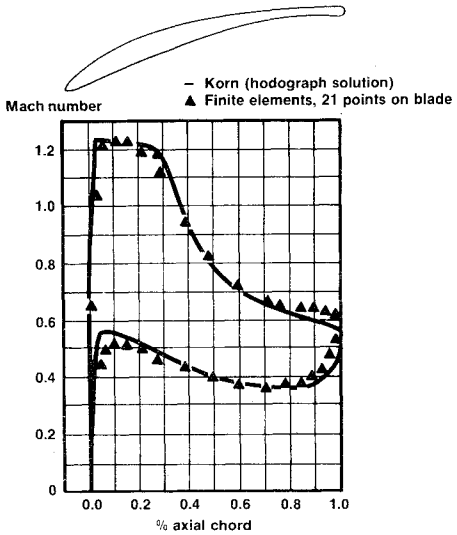

Fig. 7 FEM results for Korn supercritical cascade.

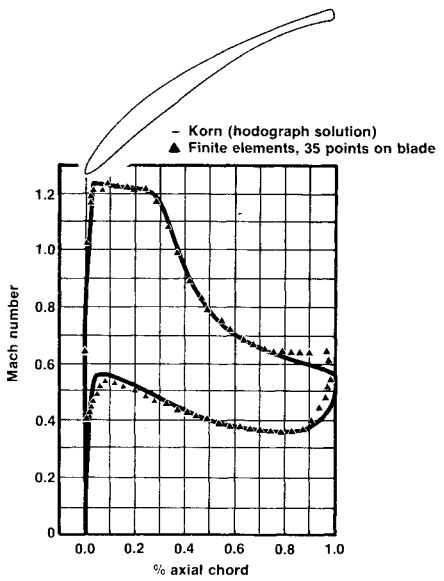

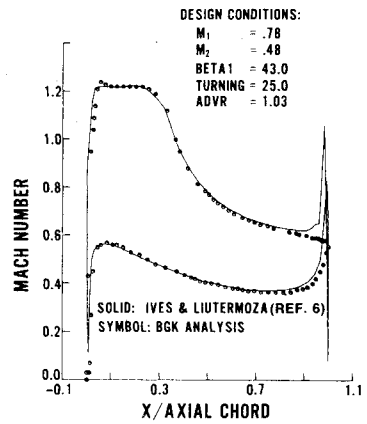

Fig. 8 FEM and FDM results for Korn supercritical cascade.

70 deg. The results obtained with 25 points on each blade surface demonstrate smoothness and uniformity of flow over the complete blade profile, even in the high gradient leading- and trailing-edge regions, and provides excellent agreement with Gostelow's exact results.

To verify the applicability to transonic test cases and indicate accuracy of the method, two test cases are presented. Both of these blade profiles were designed using hodograph methods[6,17] to provide a specified pressure distribution. Second-order accurate finite-difference solutions are also available for both blades. The first test case is a supercritical blade profile designed by Korn for shockless performance at an inlet Mach number of 0.78. We present results of the finite-element analysis in Figs. 7 and 8 with 21 points and 35 points on the blade, respectively. The results indicate a strong convergence with mesh refinement with anticipated behavior at leading and trailing edge precisely reproduced. The second-order finite-difference solution of Ives and Liutermoza[6] with 54 points on each blade surface is included for comparison. The improvement brought by finite elements over the last 25% of the blade, on both surfaces, is certainly noteworthy.

The second test case is a hodograph-designed blade of Korn and Garabedian.[5,6] The finite-element results are shown in Fig. 9. They match the design Mach number profiles to a good degree of accuracy with only 21 points on the blade.

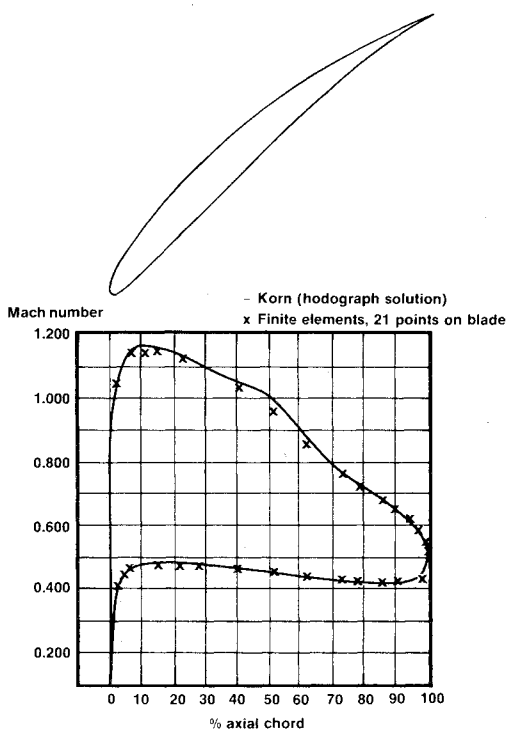

Fig. 9 FEM results for Korn-Garabedian supercritical cascade.

The finite-difference methods of Refs. 5 and 6 also compare very well. This is to be expected, however, because of the extremely low solidity (pitch/chord <0.4) and the better mapping properties of a sharp trailing edge in these particular methods.

Typical computing times are of the order of 5 to 25 s on a Cyber 170 Model 175. The interactive mesh generation program requires about 2 s of execution time on the same computer. The formulation has been kept general enough to permit the subsequent inclusion of radius change as well as streamtube contraction.

Conclusions

A novel finite-element approach to the blade-to-blade problem of turbomachines has been successfully demonstrated. The method relies on an automated mesh generation procedure using a direct, one-step explicit mapping of the blade into a near circle. Appropriate meshes are generated which give nearly equal weights to regions of high gradients at leading and trailing edges as for regions along the main body of the blade. A locally linearized variational principle, applicable to shockless transonic flows, guarantees fast convergence at or near transonic Mach numbers. Accurate solutions are obtained since the finite-element discretization is only called upon to obtain the local perturbation in each element rather than solving for the basic flow. This, however, is done with no loss in the degree of approximation of the governing differential equation.

Acknowledgments

The authors would like to acknowledge the considerable help received from V. Bhat of Pratt and Whitney in programming and automating the mesh generation scheme. This work has been partially supported by grants A-3662 and P-7901 of the Natural Sciences and Engineering Research Council of Canada.

References

[1] Katsanis, T., "Computer Program for Calculating Velocities and Streamlines on a Blade-to-Blade Stream Surface of a Turbomachine," NASA TN-D-4525, April 1968.

[2] Katsanis, T. and McNally, W. D., "Fortran Program for Calculating Velocities and Streamlines on a Blade-to-Blade Stream Surface of a Tandem Blade Turbomachine," NASA-TN-D-5044, March 1969.

[3] McDonald, P. W., "The Computation of Transonic Flow through Two-Dimensional Gas Turbine Cascades," ASME Paper No. 71-GT-89.

[4] Denton, J. D., "A Time Marching Method for Two-and Three-Dimensional Blade-to-Blade Flows," Aeronautical Research Council, R&M No. 3775, 1975.

[5] Ives, D. C. and Liutermoza, J. F., "Analysis of Transonic Cascade Flow using Conformal Mapping and Relaxation Techniques," *AIAA Journal*, Vol. 15, May 1977, pp. 647-652.

[6] Ives, D. C. and Liutermoza, J. F., "Second-Order Accurate Calculation of Transonic Flow over Turbomachinery Cascades," AIAA Paper 78-1149, Seattle, Wash., July 1978.

[7] Martin, H. C., "Finite Element Analysis of Fluid Flows," AF-FDL TR-68-150, 1968.

[8] Chan, S.T.K. and Larock, B. E., "Flows Around Cylinder between Parallel Walls," *Journal of Engineering Mechanics Division*, ASCE, Oct. 1972, pp. 1319-1322.

[9] Argyris, J. H. and Mareczek, G., "Potential Flow Analysis by Finite Elements," *Ingenieur-Archiv.*, Vol. 41, 1972, pp. 1-25.

[10] Norrie, D. H. and de Vries, G., "The Application of the Finite Element Technique to Potential Flow Problems," *Journal of Applied Mechanics*, Dec. 1971, pp. 798-802.

[11] Gelder, D., "Solution of the Compressible Flow Equations," *International Journal for Numerical Methods in Engineering*, Vol. 3, 1971, pp. 35-43.

[12] Shen, S. F. and Habashi, W. G., "Local Linearization of the Finite Element Method and its Applications to Compressible Flows," *International Journal of Numerical Methods in Engineering*, Vol. 10, 1976, pp. 565-577.

[13] Habashi, W. G., "The Finite Element Method in Subsonic Aerodynamics," *Proceedings of the 1976 Heat Transfer and Fluid Mechanics Institute*, McKillop et al. Editors, Stanford University Press, June 1976, pp. 374-389.

[14] Hirsch, C. and Warzee G., "Finite Element Computation of Subsonic Cascade Flows," *Proceedings of the 6th Canadian Congress of Applied Mechanics*, Vancouver, B.C., June 1977.

[15] Huebner, K., *The Finite Element Method for Engineers*, John Wiley and Sons, New York, 1976.

[16] Gostelow, J. P. and Smith, D.J.L., "Test Cases for Turbomachinery Flow Field Computation," CUED/A Turbo/TR 48, June 1973.

[17] Korn, D. G., "Numerical Design of Transonic Cascades," Courant Institute of Mathematical Sciences, ERDA Mathematics and Computing Laboratory, COO-3077-72, Jan. 1975.